Bolyai Institute
Faculty of Science and Informatics
University of Szeged

On a delay model of Cheyne-Stokes respiration: Computer-aided study

Thesis

Eliza Bánhegyi
Mathematics BSc

Supervisor:
Dr. János Karsai
associate professor
Department of Analysis

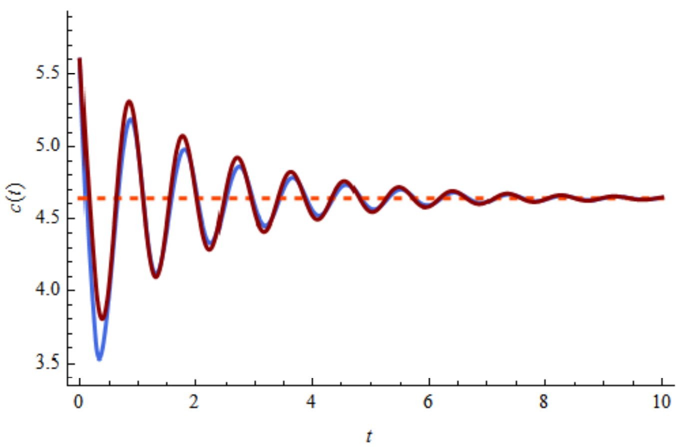

Szeged
2014

Table of contents

Acknowledgements

Hereby I am deeply grateful to my teachers for their instructions.
Foremost, I would like to express my sincere gratitude to my supervisor Dr. János Karsai for the continuous support of my thesis, for his patience, motivation and enthusiasm. His encouragement helped me a lot not only writing of this thesis but also guideing my way during years have gone by. I could not have imagined having a better supervisor and mentor for my studies.

Preface

The purpose of my thesis is to model a so-called Cheyne-Stokes respiratory ailment using delay differential equations. Based on the paper [1], we present the theoretical as well as computer-aided investigations of the model. An important aim of our work is the development of tools in Wolfram Mathematica to study the stability properties and the linearization method of delay differential equations.

On the biological relevance of differential delay equations

The use of ordinary and partial differential equations to model biological systems has a long history, dating to Malthus, Verhulst, Lotka and Volterra. As these models are used in an attempt to better our understanding of more and more complicated phenomena, it is becoming clear that the simplest models cannot capture the rich variety of dynamics observed in natural systems. There are many possible approaches to dealing with these complexities.

On one hand, one can construct larger systems of ordinary or partial differential equations, i.e., systems with more differential equations. These systems can be quite good at approximating observed behavior, but they suffer from the downfall of containing many parameters, often signifying quantities which cannot be determined experimentally. Furthermore, obtaining an intuitive sense of which components are most important in determining a behavior regime can be quite difficult.

Another approach which is gaining prominence is the inclusion of time delay terms in the differential equations. After the First World War, the development and use of automatic control systems resulted in studies of an entirely different class of differential equations these so-called delay differential equations or difference-differential equations. A time delay arises because a finite time is required to sense information and then react to it. The delays or lags can represent gestation times, incubation periods, transport delays, or can simply lump complicated biological processes together, accounting only for the time required for these processes to occur. Such models have the advantage of combining a simple, intuitive derivation with a wide variety of possible behavior regimes for a single system. On the negative side, these models hide much of the detailed workings of complex biological systems, and it is sometimes precisely these details which are of interest.

Various problems, primarily taken from many branches of biological sciences literature motivate our study of delay differential equations. It has been applied by Nicholson's careful experimental data for the Australian sheep-blowfly equation (1957). The Mackey-Glass model (1977) concerned with the regulation of haematopoiesis, the formation of blood cell elements in the body. Movement control in Parkinson's disease was studied by A. Beuter, J. G. Milton, C. Labrie, and L. Glass (1990). Furthermore, the model of the pupil light reflex is given by J.G. Milton (2003). Delay models have been commonly used for describing several aspects of infectious disease dynamics: primary infection, drug therapy and immune response, to name a few. Delays have also appeared in the study of physiology, chemostat models, circadian rhythms, economics, epidemiology, the respiratory system, tumor growth and neural networks.

We have two goals with subject of mathematical biology papers: to bring to the attention of theoreticians an example from medicine of complex and poorly understood dynamics; and to show that simple mathematical models of physiological systems predict the existence of regimes of periodic dynamics, similar to those encountered in human disease.

The structure of the thesis

Below we summarize the content of chapters of the thesis. In the first chapter we construct a model taking notice of biological aspects of the problem using Hill function. As a first step of additional work we introduce nondimensional quantities to reduce number of paramerets and simplify notations.
The second chapter concerns the existence of steady states of the equation. In addition, the linearization method of ordinary and delay differential equations are explained besides the relevant stability theorems.
Then, in the third chapter we examine the stability of equlibria depending on parameters. The bifurcation conditions of asymptotic stability are also computed. A complex figure closes this section which supports the theoretical expectations.
In the fourth chapter we give tips for interactive experiments showing typical features of the problem.
Finally, we summarize our results by comparing the experimental and computer simulated behaviours.

This thesis is an interactive *Mathematica* document which enables the reader doing dynamic experiments. It is available on the web portal www.model.u-szeged.hu.
The required Wolfram CDF-Player can be installed from the attached CD or www.wolfram.com/cdf-player/.

1. Problem: Cheyne–Stokes respiration

The Cheyne–Stokes respiration, is a human respiratory ailment manifested by an alteration in the regular breathing pattern. Here the amplitude of the breathing pattern, directly related to the breath volume — the ventilation V — regularly waxes and wanes with each period separated by periods of apnea, that is where the volume per breath is exceedingly low.

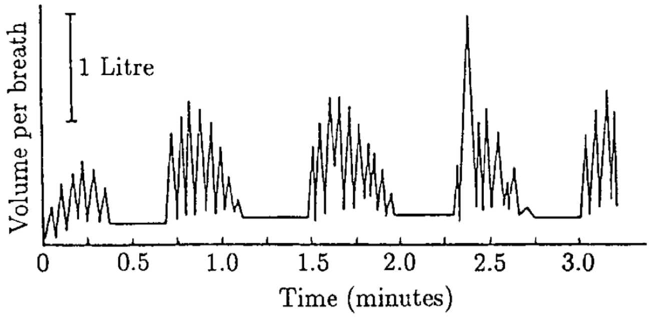

Figure 1. Typical of spirograms of those suffering from Cheyne–Stokes respiration

We first need a few physiological facts for our model. The level of arterial carbon-dioxide (CO_2), $c(t)$ say, is monitored by receptors which in turn determine the level of ventilation. It is believed that these CO_2 - sensitive receptors are situated in the brainstem so there is an inherent time lag, τ say, in the overall control system for breathing levels. It is known that the ventilation response curve to CO_2 is sigmoidal in form. We assume the dependence of the ventilation V on c to be adequately described by what is called a *Hill function*, of the form below where $V_{\max}$ is the maximum ventilation possible and the parameter a and the Hill coefficient m are positive constants which are determined from experimental data.

$$V = V_{\max} \frac{c^m(t-\tau)}{a^m + c^m(t-\tau)} \tag{1}$$

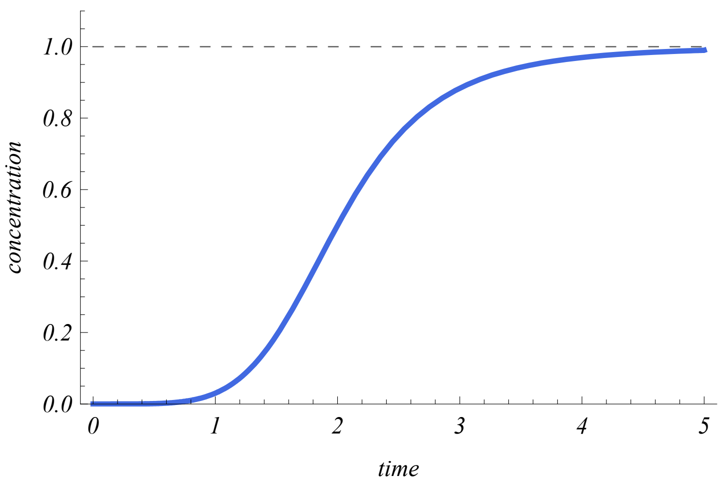

Figure 2. Hill function with $m = 5$, $a = 2$, $V_{\max} = 1$, $\tau = 0$ parameters

We assume that the removal of CO_2 from the blood is proportional to the product of the ventilation and the level of CO_2 in the blood. Let p be the constant metabolic production rate of CO_2 in the body. The dynamics of the CO_2 level is then modelled by

$$\frac{d\,c(t)}{dt} = p - b\,V\,c(t) = p - b\,V_{\max}\,c(t)\,\frac{c^m(t-\tau)}{a^m + c^m(t-\tau)}, \tag{2}$$

where b is a positive parameter which is also determined from experimental data. The delay time τ is the time between the oxygenation of the blood in the lungs and monitoring by the chemoreceptors in the brainstem. The justification for equation (2) is heuristic: the equation reproduces certain qualitative features of both normal and abnormal breathing.
As a first step in analysing (2) we introduce the nondimensional quantities

$$x = \frac{c}{a}, \qquad t^* = \frac{p\,t}{a}, \qquad \tau^* = \frac{p\,\tau}{a}, \qquad \alpha = \frac{a\,b\,V_{\max}}{p}, \qquad V^* = \frac{V}{V_{\max}}, \tag{3}$$

and the model equation becomes $x'(t) = 1 - \alpha\,x(t)\,\frac{x^m(t-\tau)}{1+x^m(t-\tau)}$,

$$x'(t) = 1 - \alpha\,x(t)\,V(x(t-\tau)), \tag{4}$$

where for notational simplicity we have omitted the asterisks on t, τ and V.

2. Steady states

2.1. Searching for steady states

We get an indication of the dynamic behaviour of solutions by investigating the linear stability of the steady state x_0 given from (4) by

$$x'(t) = 0 \Longrightarrow 1 = \alpha\,\frac{{x_0}^{m+1}}{1+{x_0}^m} = \alpha\,x_0\,V(x_0) = \alpha\,x_0\,V_0, \tag{5}$$

where V_0, defined by the last equation, is the dimensionless steady state ventilation.

THEOREM 1

There exists a unique steady state for $x'(t) = 1 - \alpha\,x_0\,V_0$ ([1] p. 23).

PROOF

Since $\frac{1}{\alpha\,x_0}$ monotonically tends to zero and $V(x_0)$ is sigmoid, and increasing to 1, as $x_0 \to \infty$, equation $\frac{1}{\alpha\,x_0} = V(x_0)$ has exactly one positive solution, being the unique positive steady state. See the illustation below.

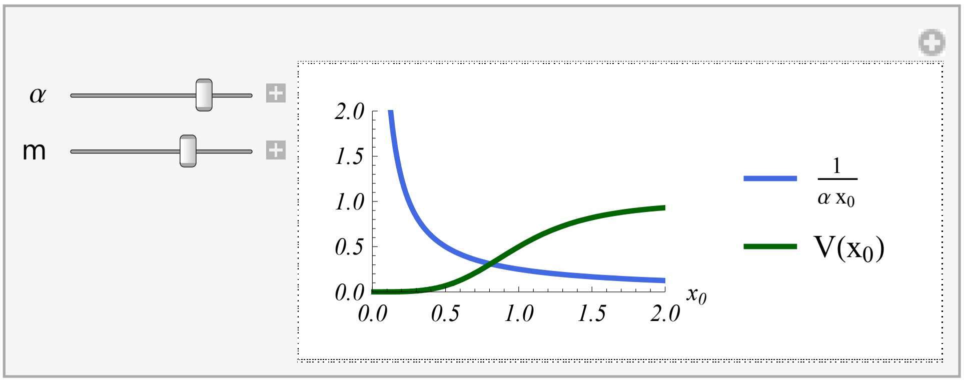

Figure 3. Existence of steady state

Determining adequately many intersection points we can frame a surface to the steady states in a function of α and m.

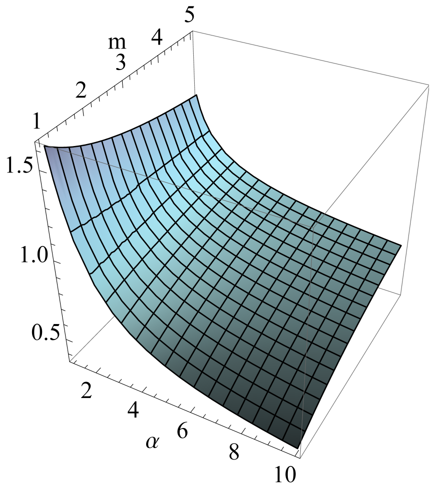

Figure 4. Surface of the steady states

2.2. On the method of linearization

The case of ODE's

Consider the following nonlinear autonomous differential equation system

$$X'(t) = F(X(t)). \tag{6}$$

It is often impossible to write down explicit solutions of a nonlinear differential equation. The one exception to this occurs when we have equilibrium solutions. Provided we can solve the algebraic equations, we can write down the equilibrium explicitly. Often, these are the most important solutions of a particular nonlinear system. More importantly, we can usually use the technique of linearization to determine the behavior of solutions near equilibrium points.

We assume that $F: D \to \mathbb{R}^n$ is continuously differentiable and $D \subset \mathbb{R}^n$ is open. Let $X(t) = X_0 \in \mathbb{R}^n$, $t \in \mathbb{R}$ is a steady-state solution of (6) if and only if $F(X_0{}^*) = 0$, where $X_0^* \in \mathbb{R}^n$ is the constant function equal to X_0. If $X(t)$ is a solution of (6) and $X(t) = X_0 + U(t)$ then $U(t)$ satisfies $U'(t) = F(X_0^* + U(t))$. We want to understand the the behavior of solutions of the last equation for solutions that start near $U = 0$. We assume that $F(X_0^* + U) = L(U) + G(U),\ U \in \mathbb{R}^n$ where $L : \mathbb{R}^n \to \mathbb{R}^n$ is a linear function and $G : \mathbb{R}^n \to \mathbb{R}^n$ is "higher order" in the sense that $\frac{|G(U)|}{||U||} \to 0,\ U \to 0$. This means that for every $\epsilon > 0$ there exists $\delta > 0$ such that $||U|| \le \delta$ implies $|G(\mathrm{U})| \le \epsilon\, \mathrm{U}$.

The approximation of F with its Taylor series around X_0 gives functions L and G. The linear system $U'(t) = L(U(t))$ is called the *linearized (or variational) equation* about the equilibrium X_0^*. The theorem below says the relationship between nonlinear and linearized systems [3] p. 151.

THEOREM 2

Consider the system $X' = F(X)$ where F is C^1. Suppose

1. $X(t)$ is a solution of $X' = F(X)$, which is defined for all $t \in [\alpha, \beta]$ and satisfies $X(t_0) = X_0$;

2. $U(t)$ is the solution to the variational equation along $X(t)$ that satisfies $U(t_0) = U_0$;

3. $Y(t)$ is the solution of $X' = F(X)$ that satisfies $Y(t_0) = X_0 + U_0$.

Then

$$\lim_{U_0 \to 0} \frac{|Y(t) - (X(t) + U(t))|}{|U_0|} = 0$$

uniformly in $t \in [\alpha, \beta]$.

Given any nonlinear system of differential equations $X' = F(X)$ with an equilibrium point at X_0, we may consider the variational equation along this solution. But DF_{X_0} is a constant matrix A. The variational equation is then $U' = L(U)$, which is an autonomous linear system. This system is called the *linearized system* at X_0. We know that flow of the linearized system is $e^{tA} U_0$, so the result above says that near an equilibrium point of a nonlinear system, the phase portrait resembles that of the corresponding linearized system. We will make the term resembles more precise in the next theorem of linearization [3] p.168.

THEOREM 3

Suppose that the n-dimensional system $X' = F(X)$ has an equilibrium point at X_0 that is hyperbolic. Then the nonlinear flow is conjugate to the flow of the linearized system in a neighborhood of X_0.

The case of DDE's

Consider the delay case of (6) $x'(t) = f(x(t), x(t-\tau))$ assuming that $f : D \times D \to \mathbb{R}$ is continuously differentiable and $D \subset \mathbb{R}$ is open. If $f(x_0, x_0) = 0$ for some $x_0 \in D$, then $x(t) = x_0$, $t \in \mathbb{R}$ is an equilibrium solution. If we now consider small perturbations about the steady state x_0 we write $u = x - x_0$ and consider $|u|$ small. We approximate f with its multivariate Taylor series around (x_0, x_0). Denote x and y the variation of f for a moment:

$$f(x, y) = f(x_0, x_0) + J(x_0).(u(t), u(t-\tau)) + O\left(u^2\right). \tag{7}$$

where $J(x_0) = (\partial_x f, \partial_y f)(x_0, x_0)$. Hence, the linearized equation is $u'(t) = J(x_0).(u(t), u(t-\tau))$.

2.3. Linearization of our DDE

Applying the above general method to equation $x'(t) = 1 - \alpha\, x(t)\, V(x(t-\tau))$, we have $f(x, y) = 1 - \alpha\, x\, V(y)$, and the partial derivatives are $(\partial_x f, \partial_y f)(x_0, x_0) = (-\alpha\, V(x_0), -\alpha\, x_0\, V'(x_0))$. It follows that the linearized equation is

$$u'(t) = A\, u(t) + B\, u(t-\tau). \tag{8}$$

where $A = -\alpha\, V(x_0) < 0$, $B = -\alpha\, x_0\, V'(x_0) < 0$.
We look for solutions in the form $u(t) \propto e^{\lambda t}$ as in the ordinary case. Substituting it to (8) we get $\lambda e^{\lambda t} = A\, e^{\lambda t} + B\, e^{\lambda (t-\tau)}$. Simplifing both sides with the positive $e^{\lambda t}$, the characterstic equation - which is transcendental - is

$$\lambda = A + B\, e^{-\lambda \tau}. \tag{9}$$

As an observation, h defined by $h(\lambda) = \lambda - A - B\, e^{-\lambda \tau}$, is an analytic function defined for all $\lambda \in \mathbb{C}$, that is, an entire function, analytic in the entire complex plane. Properties of nontrivial entire functions, in particular of h, are listed below :

- Each characteristic root has finite order.
- There are at most countably many characteristic roots.
- The set of characteristic roots has no finite accumulation point.

Consider the characteristic equation (9). By product both sides with $e^{\lambda \tau}$ and rearranging we get a so-called product logarithm or Lambert W function $B = (\lambda - A)\, e^{\lambda \tau}$. There are 4 kinds of solution to this equation respect to λ: $B = -A$ and $\lambda = 0$, $\tau = 0$ and $\lambda = A + B, \tau \neq 0$ and $B = 0$ and $\lambda = A$, $c \in$ Integers and $\tau \neq 0$ and $B\,\tau \neq 0$ and $\lambda = \frac{A\,\tau + \text{ProductLog}[c, B\, e^{-A\,\tau}\,\tau]}{\tau}$. With conditions on A, B and τ the fourth expression give us the eigenvalues.

Figure 5 shows some characterstic roots of equation (9) depending on the parameters, where n denotes the n^{th} solution of the above mentioned product logarithm function. Notice that roots come in complex conjugate pairs (see [2] p. 47).

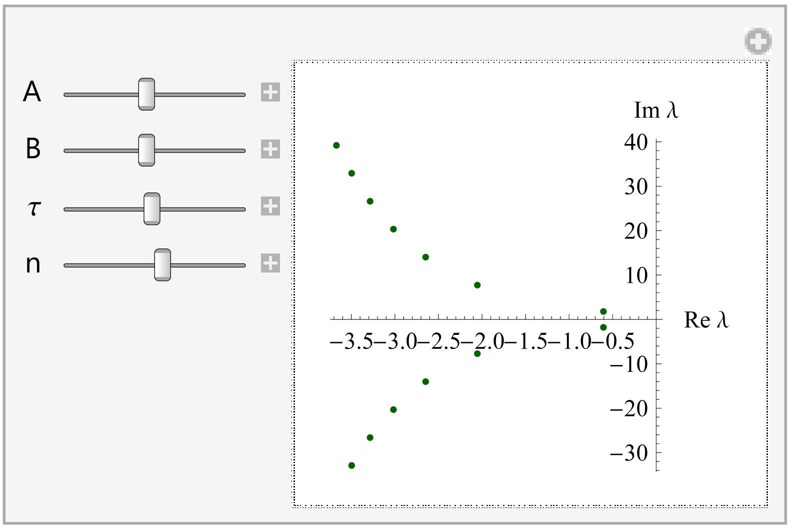

Figure 5. Some roots of the characteristic equation

The following theorem ([2] p. 55) can be formulated:

THEOREM 4

Let $h(\lambda) = 0$ *denote the characteristic equation corresponding to (8) and suppose that* $\mu_0 := \max_{h(\lambda)=0} \operatorname{Re} \lambda < 0$. *Then* $x_0{}^*$ *is a locally asymptotically stable steady state of (4). In fact, there exists* $\delta > 0$ *such that*

$$\|u - x_0{}^*\| < \delta \Longrightarrow \|x(t+u) - x_0{}^*\| \leq K\, \|u - x_0{}^*\|\, e^{-\frac{\mu_0 t}{2}},\ \ t \geq 0.$$

If $\operatorname{Re} \lambda > 0$ *for some characteristic root, then* $x_0{}^*$ *is unstable.*

3. Stability of equlibrium

3.1. On the general equation $u'(t) = A\,u(t) + B\,u(t-\tau)$

We obtain a complete picture of the characteristic roots associated with the linearized equation $u'(t) = A\,u(t) + B\,u(t-\tau)$ in the case that A and B are real scalars. As we got before, the characteristic equation is $\lambda = A + B\,e^{-\lambda\tau}$.
Taking $\lambda = \mu + i\nu$, Eulers's formula gives

$$\begin{aligned} \mu &= A + B\,e^{-\mu\tau} \cos \nu\tau \\ \nu &= -B\,e^{-\mu\tau} \sin \nu\tau \end{aligned} \tag{10}$$

Observe that $\lambda = 0$ is a root precisely when $A + B = 0$, see *Figure 6* below.

Define the function $F(\lambda, A, B) := \lambda - A - B\,e^{-\lambda\tau}$ whose zeros are the roots of (9). One of our main tasks in determining the stability of an equilibrium solution is to understand the characteristic roots of an analytic characteristic equation $h(\lambda) = 0$. In practice, there are usually important parameters, such as the delay, and we would like to know how the roots vary with the parameters. Therefore, we must study the roots λ of the equation $h(\lambda, p) = 0$ where p denotes a vector of usually real parameters. For solutions (λ_0, A_0, B_0) of (9), the implicit function theorem guarantees a smooth root $\lambda = \lambda(A, B)$ for (A, B) near (A_0, B_0).

Setting $\mu = 0$ in (10) and solving for α and β gives the "neutral stability curves" in parameter space along which (9) has purely imaginary roots $\lambda = i\,\nu$.
Multiply by τ will simplify our notations, let $z = \lambda\,\tau$, $\alpha = A\,\tau$, $\beta = B\,\tau$, $y = \nu\,\tau$ to obtain $z = \alpha + \beta\,e^{-z}$.

As roots come in complex conjugate pairs, we may restrict $y \geqslant 0$. Notice that the curve is well-defined at $y = 0$ where $(\alpha, \beta) = (1, -1)$, which coincides with the parameter values at which $z = 0$ is a double root. (By the way, there are no roots of order three or higher. [2] p. 58.) We denote the curve by

$$C_0 := \left\{(\alpha, \beta) = \left(y\,\frac{\cos y}{\sin y}, -y\,\frac{1}{\sin y}\right), 0 \leqslant y < \pi\right\}$$

along which $z = \pm i\,y$, $0 \leqslant y < \pi$ are roots. It is depicted in *Figure 6* below. Calculations give

$$\frac{d\,\alpha}{dy} < 0, \;\; \frac{d\,\beta}{dy} < 0, \;\; 0 < y < \pi$$

so both $\alpha(y)$, $\beta(y)$ decrease with increasing y. Starting from $(1, -1)$ when $z = 0$, $(\alpha(y), \beta(y))$ meets the β-axis at $(0, \frac{\pi}{2})$ when $z = \frac{\pi}{2}$. It then enters the third quadrant and approaches $(-\infty, \infty)$ from below and tangent to the line $\alpha = \beta$ as $y \nearrow \pi$ because $\frac{\alpha}{\beta} = -\cos(y) \to 1$ whereas both $\alpha, \beta \to -\infty$ as $y \nearrow \pi$.We also need to consider the curves

$$C_n := \left\{(\alpha, \beta) = \left(y\,\frac{\cos y}{\sin y}, -y\,\frac{1}{\sin y}\right), n\,\pi \leqslant y < (n+1)\,\pi\right\}, \;\; n \geqslant 1,$$

where $z = \pm i\,y$, $n\,\pi < y < (n+1)\,\pi$, are roots. Notice that $(-1)^n \sin y > 0$ on $n\,\pi < y < (n+1)\,\pi$ so $(-1)^{n+1}\,\beta > 0$ on C_n but α changes sign at $y = n\,\pi + \frac{\pi}{2}$. On C_n, $\frac{d\,\alpha}{dy} < 0$ but $\frac{d\,\beta}{dy}$ changes sign on $(n\,\pi, (n+1)\,\pi)$, where $\tan y = y$. Because $\frac{\beta}{\alpha} = -\frac{1}{\cos y}$, $\left|\frac{\beta}{\alpha}\right| > 1$ on C_n implying that C_1, C_3, ... lie strictly above the graph of $\beta = |\alpha|$ and C_2, C_4, ... lie strictly below the graph of $\beta = -|\alpha|$.

It is easy to see that $C_{2\,n+1}$ lies strictly above $C_{2\,n-1}$ for $n = 1, 2, \ldots$ and that $C_{2\,(n+1)}$ lies strictly below $C_{2\,n}$ for $n = 1, 2, \ldots$. C_n never meets C_0, the line $\alpha + \beta = 0$, nor the open region enclosed by these two curves.

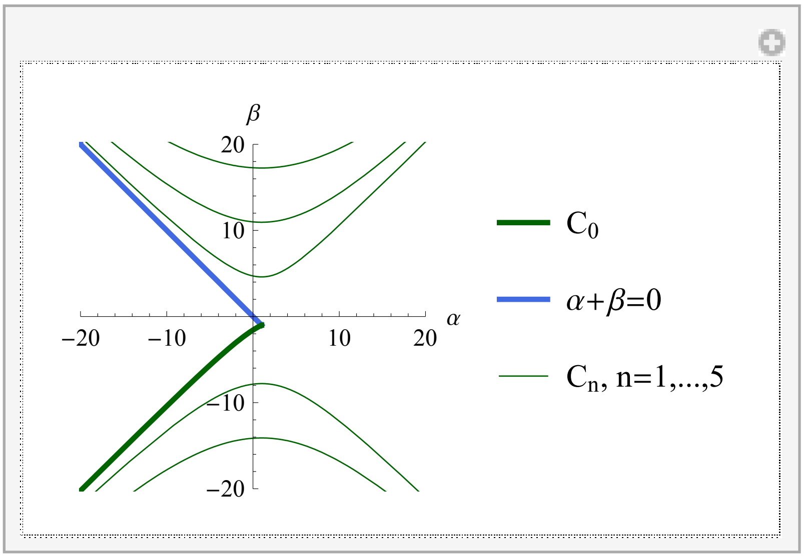

Figure 6. Neutral stability curves

THEOREM 5

All roots of (9) have Re $\lambda < 0$ for (α, β) belonging to the open region bounded below by curve C_0 and bounded above by curve $\{(\alpha, \beta) : \beta = -\alpha, \alpha \leqslant 1\}$ which meet at $(\alpha, \beta) = (1, -1)$. See Figure 6. At least one root satisfies Re $\lambda > 0$ for (α, β) belonging to the open complementary region on the right. [2] p. 52

Now let’s return to our original problem of determining the stability of the steady state $u = 0$ of linearized equation (8) which depends on characteristic equation (9). We assume that $A + B \neq 0$ for otherwise $\lambda = 0$ is a root. The theorem below states stability conditions for the variational equation [2] p. 53:

THEOREM 6

The following hold for (8)*:*
(a) If $A + B > 0$, then $u = 0$ is unstable.
(b) If $A + B < 0$ and $B \geq A$, then $u = 0$ is asymptotically stable.
(c) If $A + B < 0$ and $B < A$, then there exists $\tau_c > 0$ such that $u = 0$ is asymptotically stable for $0 < \tau < \tau_c$ and unstable for $\tau > \tau_c$.
In case (c), there exist a pair of purely imaginary roots at $\tau_c = \frac{1}{\sqrt{B^2 - A^2}} \frac{1}{\cos\left(-\frac{A}{B}\right)}$.

3.2. The special case of Cheyne-Stokes respiration

We found above that if the solution λ of the characteristic equation with the largest real part is negative, then the steady state is asympotically stable. Hence we are concerned with the oscillatory nature of the disease we are interested in parameter ranges where the steady state is unstable and, in particular, unstable by growing oscillations in anticipation of limit cycle behaviour. So, we must determine the bifurcation values of the parameters such that $\operatorname{Re}\lambda = 0$.

Simultaneous solutions of (10) give μ and ν in terms of A, B and τ but we cannot determine them explicitly. The bifurcation we are interested in is when $\mu = 0$ so we consider the parameter ranges which admit such a solution. With $\mu = 0$ euqations (10) give, with

$$\operatorname{ctg} \nu\tau = \frac{A\,\tau}{\nu\tau}, \qquad \frac{\pi}{2} < (\nu\tau)_1 < \pi, \tag{11}$$

for all finite $A < 0$ where $(\nu\tau)_1$ is a solution. We can see that such a solution $(\nu\tau)_1$ exists on sketching $\operatorname{ctg} \nu\tau$ and $\frac{A\,\tau}{\nu\tau}$ as functions of $\nu\tau$.

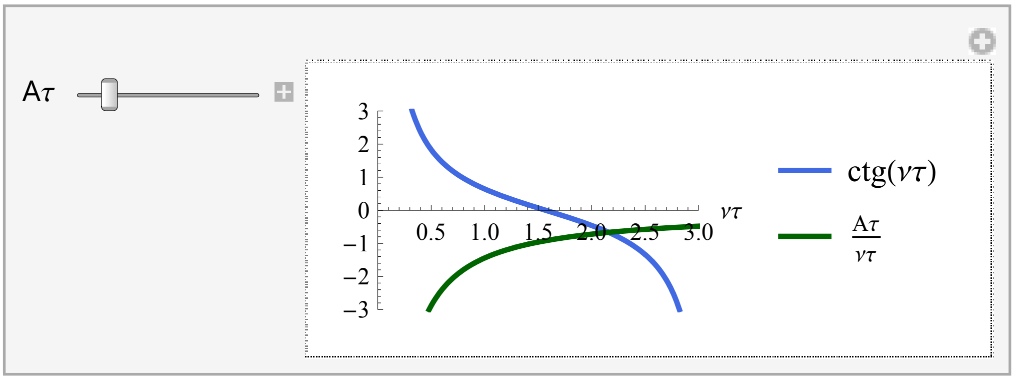

Figure 7. Existence of solution $(\nu\tau)_1$on the interval $\left(\frac{\pi}{2}, \pi\right)$

Obviously, there are other solutions $(\nu\tau)_m$ of this equation in the ranges $\left[(2\,m+1)\,\frac{\pi}{2},\,(m+1)\,\pi\right]$ for $m = 1, 2, \ldots$ but we need only to consider the smallest positive solution $(\nu\tau)_1$ since that gives the bifurcation for the smallest critical $\tau > 0$. We now have to determine the parameter ranges so that with $\mu = 0$ and $\nu\tau$ substituted back into (10) a solution exists. That is, what are the restrictions on A, B and τ so that

$$\begin{aligned} 0 &= A + B\cos(\nu\tau)_1, \\ (\nu\tau)_1 &= -B\,\tau\sin(\nu\tau)_1 \end{aligned}$$

are consistent? These imply

$$-B\,\tau = \sqrt{(-A\,\tau)^2 + (\nu\tau)_1{}^2}\,. \tag{12}$$

If A, B and τ, which determine $(\nu\tau)_1$, are such that the last equality cannot hold then no solution with $\mu = 0$ exists.

Since A and B are negative, the solution is stable in the limiting case $\tau = 0$ since then $\mathrm{Re}\,\lambda = \mu = A + B < 0$. Now consider (10) and increase τ from $\tau = 0$. From the last equation and (11) a solution with $\mu = 0$ cannot exist if

$$\begin{gathered} -B\,\tau < \sqrt{(-A\,\tau)^2 + (\nu\tau)_1{}^2} \\ (\nu\tau)_1 \operatorname{ctg}(\nu\tau)_1 = A\tau, \quad \tfrac{\pi}{2} < (\nu\tau)_1 < \pi \end{gathered} \tag{13}$$

and, from continuity arguments from $\tau = 0$ we must have $\mu < 0$. So the bifurcation condition which just gives $\mu = 0$ is (12). Or, put in another way, if (13) holds, the steady state solution of (4) is linearly, and in fact globally, asymptotically stable. In terms of the original dimensionless variables the conditions are thus

$$\begin{gathered} \alpha\, x_0\, V_0'\,\tau < \sqrt{(\alpha\, V_0\,\tau)^2 + (\nu\tau)_1{}^2}\,, \\ (\nu\tau)_1 \operatorname{ctg}(\nu\tau)_1 = -\alpha\, V_0\,\tau \end{gathered}$$

If we now have A and B fixed, a bifurcation value τ_c is given by (12).

Actual parameter values for normal humans have been obtained by Mackey and Glass (1977). The concentration of gas in blood is measured in terms of the partial pressure it sustains and so it is measured in mmHg (that is, in torr). Dalton's law states that the partial pressure exerted by each gas in a mixture equals the total pressure times the individual composition of the gas in the mixture. Relevant to the dimensional system (2), they estimated $V_0 = 7$ litre / min, the average ventilation per minutes, which is the product of the tidal volumen (half litre) and the sedent breathing frequency (14/min), $c_0 = 40$ mmHg, $p = 6$ mmHg / min, $V_0' = 4$ litre / min mmHg, $\tau = 0.25$ min.

From (5), which defines the dimensionless steady state, we have $\alpha\, V_0 = \frac{1}{x_0}$. So, with the stability condition in mind, we have, using the nondimensionalisation,

$$-A\,\tau = \alpha\, V_0\,\tau = \frac{\tau}{x_0} = \frac{p\,\tau_{\text{dimensional}}}{c_0} = \frac{6 \times 0.25}{40} = 0.0375.$$

The solution of the second of (13) with such a small right-hand side is $(\nu\tau)_1 \approx \frac{\pi}{2}$ and so $(\nu\tau)_1 \gg \alpha\, V_0\,\tau$ which means that the inequality for stability from the dimensionless stability condition is approximately, but quite accurately, $V_0' < \frac{\pi}{2\,\alpha\, x_0\,\tau}$. So, if the gradient of the ventilation at the steady state becomes too large the steady state becomes unstable and limit cycle periodic behaviour ensues. With the estimated parameter values the critical dimensional ventilation is

$$V_0' = \frac{\pi}{2\,\alpha\, x_0\,\tau} = \frac{\pi\, V_0}{2\,\tau} \text{ (dimensionless values)} \Longrightarrow \frac{V_0'}{V_{\max}} = \frac{\pi\, V_0}{2\, p\,\tau_{\dim}\, V_{\max}} \text{ (dimension values)}$$

$$\Longrightarrow V_0' = \frac{\pi\, V_0}{2\, p\,\tau_{\dim}} = \frac{\pi\, 7}{2 \times 6 \times 0.25} \approx 7.33 \text{ litre / min mmHg}$$

The gradient increases with the Hill coefficient m. Other parameters can of course also initiate periodic behaviour; all we require is that $V_0' < \frac{\pi}{2\,\alpha\, x_0\,\tau}$ is violated. In

dimensional terms we can determine values for m and a in the expression (1) for the ventilation, which result instability.
As either the steepness of the CO_2 response or the delay time increases, the steady states becomes unstable and low amplitude oscillations or high amplitude oscillations in which there is distinct apnea are observed. Similar breathing patterns are observed clinically. Cheyne-Stokes respiration is often found in patients who have increased delay times between oxygenation of the blood in the lungs and stimulation of chemoreceptors in the brainstem, and also increased sensitivity to CO_2. A phenomenon analogous to Cheyne-Stokes respiation in humans has been induced in dogs by inserting a circulatory delay between the heart and the brain. There are other pathological conditions in which highly irregular breathing patterns are observed; for example apneic breathing in premature infants.

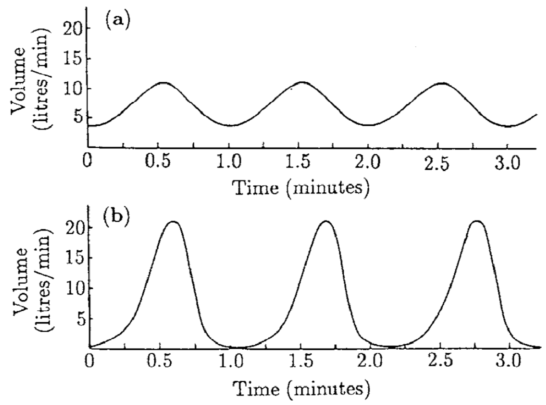

Figure 8. Dimensional results of numerical simulations of
$c'(t) = p - b\, V_{\max}\, c(t)\, \frac{c^m(t-\tau)}{a^m + c^m(t-\tau)}$ in [1]

Figures 8 (a) and (b) show the dimensional results of numerical simulations of (2) with $V_0' = 7.7$ litre / min mmHg and $V_0' = 10.01$ litre / min mmHg. Note that the period of oscillation in both solutions is about 1 minute, which is 4τ where $\tau = 0.25$ min is the estimate for delay given in human parameters.
These analytical results are similar to results found by numerical integration of more complex models of the respiratory system. Because of the crudeness of our mathematical model and experimental difficulties encountered in measuring respiratory control parameters, detailed numerical comparision with experiments are difficult. However our value for τ is comparable to that found in Cheyne-Stokes patients. Our critical value for V_0 lies above the generally accepted normal range of 2 to 6 liter/min mmHg, and is comparable to sensitivities found in Cheyne-Stokes patients. The experimentally observed period of Cheyne-Stokes breathing is of the order two or three times the estimated τ.

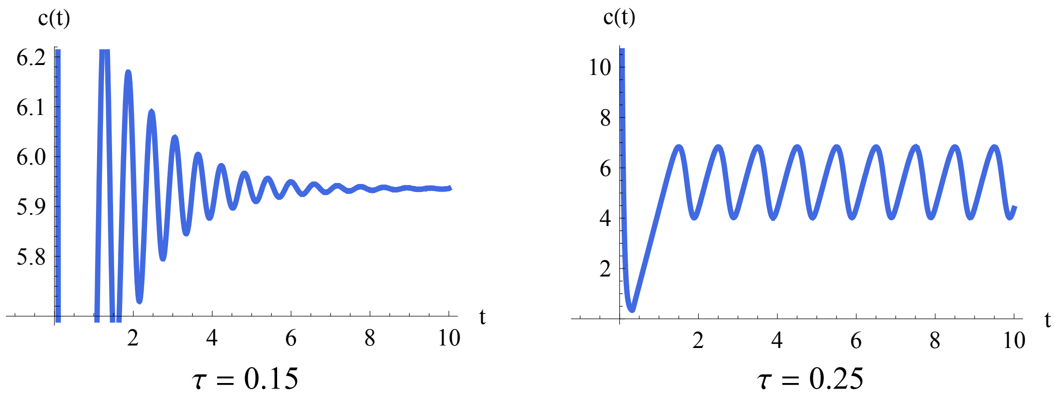

Figure 9. Solution of $c'(t) = p - b\,V_{\max}\,c(t)\,\frac{c^m(t-\tau)}{a^m + c^m(t-\tau)}$

Figure 9 shows the solution with two different τ. On the first one we can see the oscillation dying out because $\tau < \tau_c$, the second one shows periodicity with $\tau > \tau_c$.

4. Computer-aided experiments

The undermentioned figures support the theoretical results. Shifting the solution curve of linearized equation to the steady state it has similar behaviour than nonlinearized one.

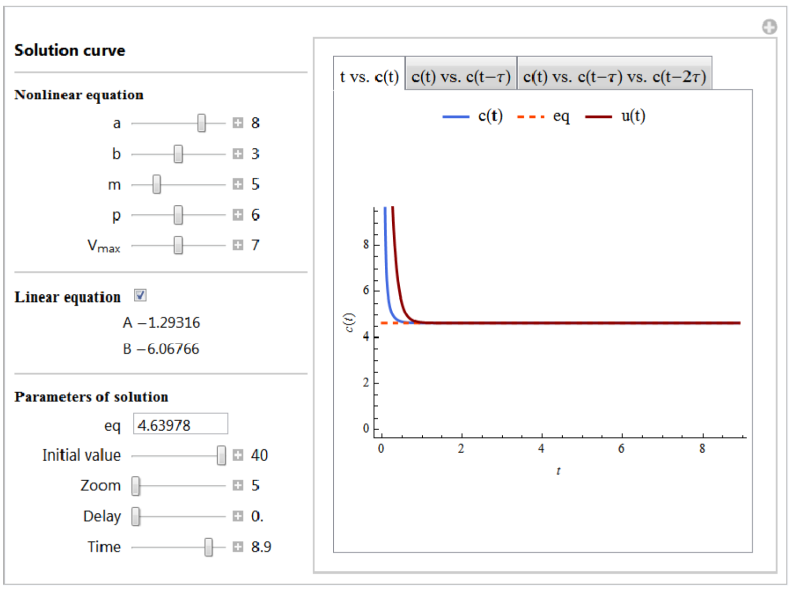

Figure 10. ODE case, Iv = 40, Zoom = 5, Delay = 0, Time = 8.9

Considering the equations without delay ($\tau = 0$) both curves quickly, monotonically decrease to the equlibrium. What would happen if we vary conditions? Nothing. Changes neither in nonlinear equation parameters nor in the initial value will modify the curves, only the monotonic behaviour is different compared to the steady state. In this case we deal with ordinary differential equation (*Figure 10)*.

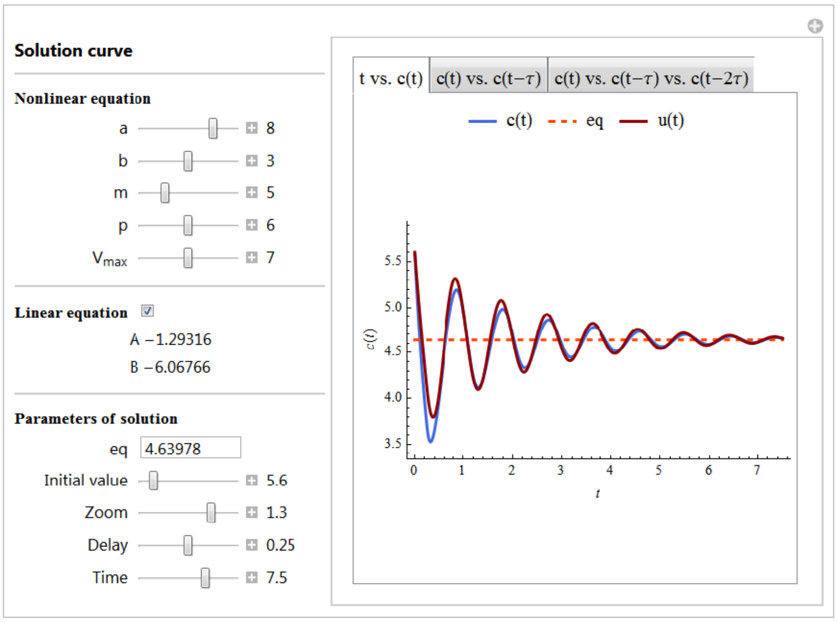

Figure 11. Asymptotic stability t *vs.* $c(t)$, Iv = 5.6, Zoom = 1.3, Delay = 0.25, Time = 7.5

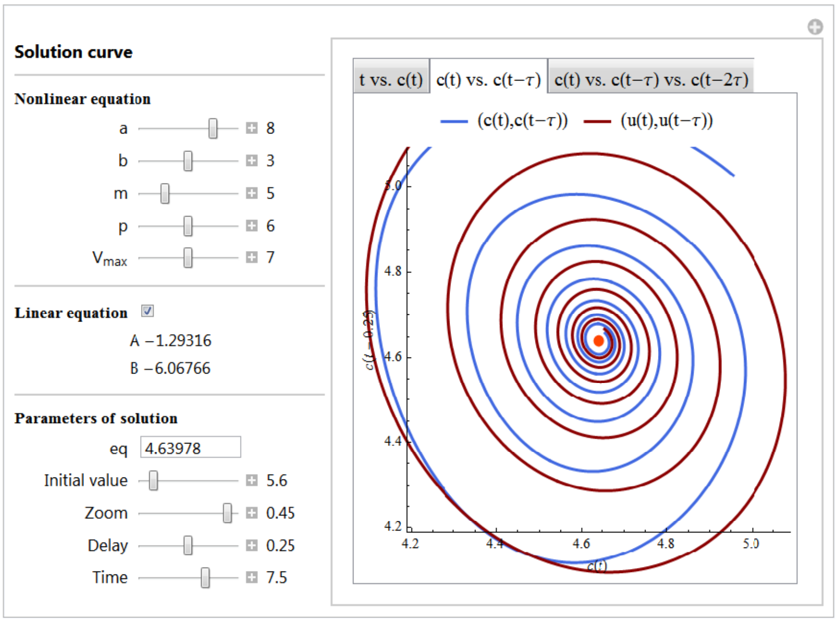

Figure 12. Asymptotic stability $c(t)$ *vs.* $c(t-\tau)$, Iv = 5.6, Zoom = 0.45, Delay = 0.25, Time = 7.5

Set the delay $\tau = 0.25$. The oscillation around the steady state will die out, asymptotic stability appears. The linearized curve follows the original one with small perturbation. In function of $c(t)$ *vs.* $c(t-\tau)$ also attractive behaviour shows up. Both tend to the steady state which is a point with same coordinates (does not depend on delay). The initial value determines the amplitude and the length of oscillation in time. Lets modify it. An interesting option is 6. The curves move close together almost write the same lines. Higher or lower settings are similar to the represented one *(Figure 11-12)*.

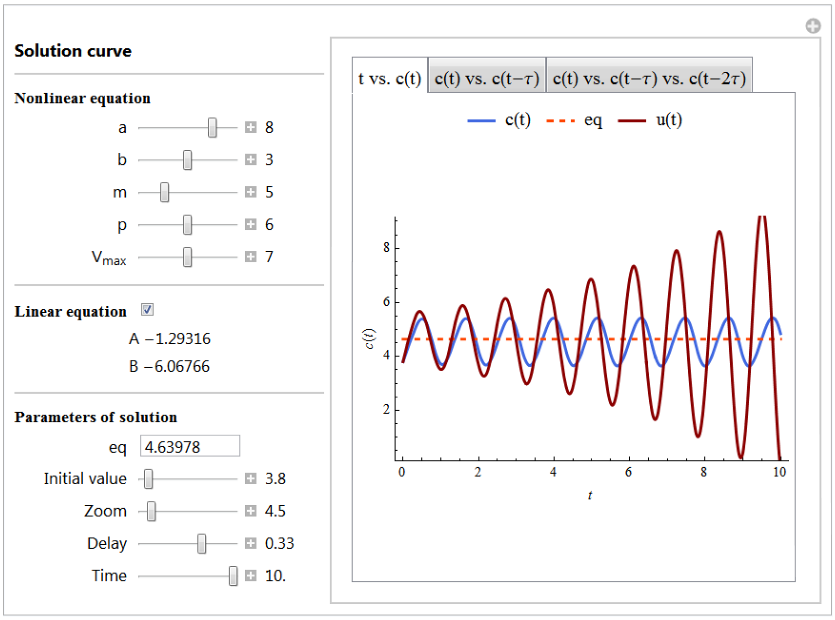

Figure 13. Stability-instability t *vs.* $c(t)$, Iv = 3.8, Zoom = 4.5, Delay = 0.33, Time = 10

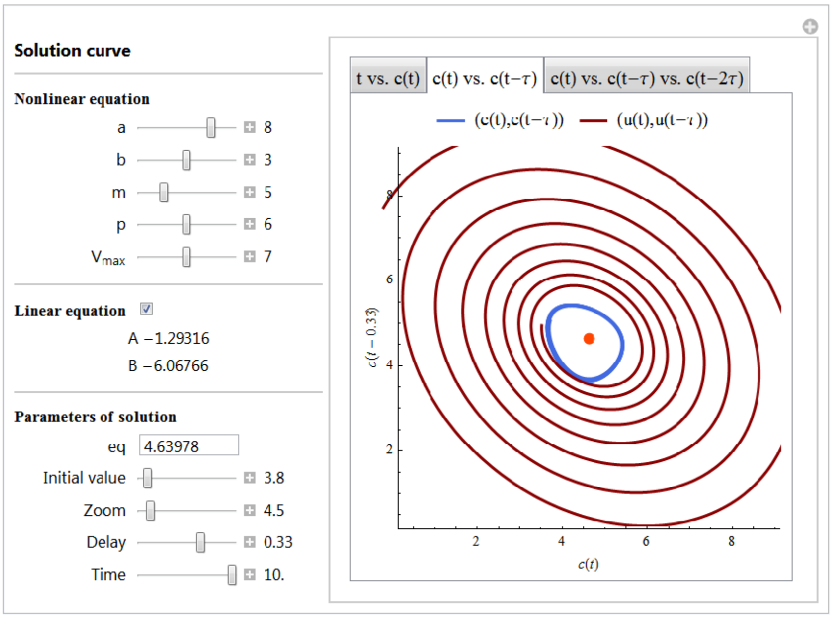

Figure 14. Stability-instability $c(t)$ *vs.* $c(t-\tau)$, Iv = 3.8, Zoom = 4.5, Delay = 0.33, Time = 10

Exceeding the critical delay bounded periodic behaviour shows up in the dimensional solution. The solutions start strictly together then they separate from each other. The linearized one differs more and more with from the steady state with growing amplitude *(Figure 13-14)*.

Emerging questions:

– Is there an option of parameters when both solutions are stable with limit cycle oscillation?
– Is there an option of parameters when both solutions are instable at the same time?
– Which parameter causes the least and the biggest difference in the shape of curves?

5. Summary

The purpose of this thesis is to do computer-aided investigations of the stability properties of equilibria of delay differential equations features via a so-called Cheyne-Stokes respiratory ailment.

Based on work of J. D. Murray in Mathematical Biology p. 21 we defined a model which describes the biologicalphenomenon and nondimensionalized it for further studies. The existence of equlibrium are stated also computable knowing the adequate parameters. We sumarized the linearization method of ordinary differential equations as well delay differential equation. We investigated the solution of linearized equation in the form of $e^{\lambda t}$ even as ordinary case. The characteristic equation has distinct features as in ordinary case. There are at most countably many characteristic roots and the set of characteristic roots has no finite accumulation point. On the general equation $u'(t) = A\,u(t) + B\,u(t-\tau)$ we determined the neutral stability curves along which the characteristic equation has purely imaginary roots. Since here we are concerned with the oscillatory nature of the disease we were interested in parameter ranges where the steady state is unstable so, we must determined the bifurcation values of the parameters such that $\mathrm{Re}\,\lambda = 0$. As a summary of our theoretical statements the last complex interactive figure lets us experiment with parameter ranges, initial condition and delay time of the problem.

We have shown how simple mathematical model of a physiological control systems can reproduce qualitative features of normal and pathological functions. We believe there is a large class of dynamical diseases, one of which have been considered here, characterised by the operation of a basically normal control system in a region of physiological parameters that produces pathological behaviour. Our analysis suggest the following approaches: demonstrate the onset of abnormal dynamics in animal models by gradual tuning of control parameters; gather sufficiently detailed experimental and clinical data to determine whether sequences of bifurcations similar to those found here actually occur in physiologycal systems; and attempt to devise novel therapies for disease by manipulating control parameters back into the normal range.

Finally, we mention that an important result of our work is the development of tools in Wolfram *Mathematica* to study the stability properties and the linearization method of delay differential equations.

References

[1] J. D. Murray, Mathematical Biology, Springer, 2002

[2] Hal Smith, An Introduction to Delay Differential Equations with Applications to the Life Sciences, Springer, 2010

[3] Morris W. Hirsch, Stephen Smale, Robert L. Devaney, Differential Equations, Dynamical Systems, and an Introduction to Chaos, Elsevier, 2003

[4] Jonathan Erwin Forde, Delay Differential Equation Models in Mathematical Biology, The University of Michigan, 2005

[5] Thomas Erneux, Applied Delay Differential Equations, Springer, 2009

[6] Yang Kuang, Delay Differential Equations: With Applications in Population Dynamics, Academic Press, 1993

[7] M.C. Mackey, L. Glass, Oscillation and chaos in physiological control systems, Science, New Series, Volume 197, p. 287-289, 1977

[8] http://www.wolfram.com/

[9] http://www.demonstrations.wolfram.com/

[10] Electronic supplement of this thesis: http://www.model.u-szeged.hu/index.php?action=edoc&cmd=show_edoc&edoc_id=31

A. Appendix

Notations

$c(t)$: concentration of CO_2 in arteries
$x(t)$: dimensionless concentration
$u(t)$: linearized variable
t: time
τ: delay
λ: eigenvalues of the characteristic equation
μ: real part of λ
ν: imaginary part of λ

DEFINITION 1

A *delay differential equation* is a differential equation where the time derivatives at the current time depend on the solution and possibly its derivatives at previous times :

$$\begin{cases} x'(t) = F(t, x(t), x(t-\tau_1), \ \ldots, x(t-\tau_n), \ \ldots, x'(t-\sigma_1), \ \ldots, \ x'(t-\sigma_m)), \\ \qquad t \geqslant t_0 \\ x(t) = \phi(t), \ t \leqslant t_0 \end{cases}$$

Instead of a simple initial condition, an initial (history) function $\phi(t)$ needs to be specified. The quantities $\tau_i \geqslant 0, \ i = 1, \ ..., n$ and $\sigma_i \geqslant 0, \ i = 1, \ ..., m$ are called the delays or time lags. The delays may be constants, functions $\tau(t)$ and $\sigma(t)$ of t (time-dependent delays), or functions $\tau(t - x(t))$ and $\sigma(t - x(t))$ (state-dependent delays).
A time-dependent solution of a DDE is not uniquely determined by its initial state at a given moment but, instead, the solution profile on an interval with length equal to the delay (or time lag) τ has to be given. That is, we need to define an infinite-dimensional set of initial conditions between $t = -\tau$ and $t = 0$. Thus, DDEs are infinite-dimensional problems, even if we have only a single linear DDE.

DEFINITION 2

We say that f is an *analytic function* on D provided D is an open set and f is differentiable at each point of D, besides if f is analytic on all of $\mathbb{C}$ then f is said to be an *entire function*.

B. Appendix

Figure 2

```
Manipulate[Plot[{c^m/(a^m + c^m), 1}, {c, 0, 5}, PlotRange → {0, 1.1},
   PlotStyle → {{Thick, ColorData["HTML"]["RoyalBlue"]},
     {ColorData["HTML"]["DimGray"], Dashed}},
   Frame → {True, True, False, False},
   FrameLabel → {"time", "concentration"},
   FrameStyle → {Italic, Italic}, ImageSize → 140],
  {{m, 5}, 1, 10, ControlPlacement → Left, ImageSize → Tiny},
  {{a, 2}, 0, 10. ControlPlacement → Left, ImageSize → Tiny},
 ControlPlacement → Left]
```

Figure 3

```
Manipulate[Module[{rhs = 1/(α x0), lhs = x0^m/(1 + x0^m)},
   Plot[{rhs, lhs}, {x0, 0, 3}, PlotRange → {{0, 2}, {0, 2}},
    PlotStyle → {{Thick, ColorData["HTML"]["RoyalBlue"]},
      {Thick, ColorData["HTML"]["DarkGreen"]}},
    AxesLabel → {"x₀"}, AxesStyle → {Italic, Italic},
    PlotLegends → {"1/(α x₀)", "V(x₀)"}, ImageSize → 140]],
  {{α, 4}, .1, 5}, {{m, 3}, 1, 5}, ControlPlacement → Top]
```

Figure 4

```
es = Flatten[
    Table[{α, m, FindRoot[1/(α x0) == x0^m/(1 + x0^m), {x0, 0.5}][[1, 2]]},
     {α, 1, 10, 0.1}, {m, 1, 5, 0.1}], 1];
f = Interpolation[es];
Plot3D[f[α, m], {α, 1, 10}, {m, 1, 5}, BoxRatios → 1,
 ColorFunction → ColorData["AtlanticColors"],
 AxesLabel → {"α", "m"}, ImageSize → 150]
```

Figure 5

```
Manipulate[
 DynamicModule[{},
  ListPlot[{
    Table[Tooltip[1/τ (A τ + ProductLog[c, B ⅇ^(-A τ) τ])],
     {c, -n, n}] /. z_?NumericQ → {Re[z], Im[z]}},
   AxesLabel → {"Re λ", "Im λ"}, AspectRatio → 1,
   AxesOrigin → {0, 0}, PlotStyle →
    {{ColorData["HTML"]["DarkGreen"], PointSize[0.02]}},
   ImageSize → → 150]
 ], {{A, -1}, -10, 10, ImageSize → Tiny},
 {{B, -1}, -10, 10, ImageSize → Tiny},
 {{τ, 1.}, 0.1, 2, ImageSize → Tiny},
 {{n, 8}, 1, 10, 1, ImageSize → Tiny}, ControlPlacement → Left]
```

Figure 6

```
Manipulate[Show[{ParametricPlot[{α, -α},
     {α, -20, 1}, PlotRange → {{-20, 20}, {-20, 20}},
     PlotStyle → {Thick, ColorData["HTML"]["RoyalBlue"]},
     PlotLegends → {"α+β=0"},
     AxesLabel → {"α", "β"}, ImageSize → 150],
    ParametricPlot[{s Cos[s]/Sin[s], -s 1/Sin[s]},
     {s, .1, π - .1}, PlotRange → {{-20, 20}, {-20, 20}},
     PlotStyle → {ColorData["HTML"]["DarkGreen"], Thick},
     PlotLegends → {"C₀"}],
    ParametricPlot[{s Cos[s]/Sin[s], -s 1/Sin[s]},
     {s, .1, (n + 1) π - .1}, Exclusions → {Sin[s] == 0},
     PlotRange → {{-20, 20}, {-20, 20}},
     PlotStyle → ColorData["HTML"]["DarkGreen"],
     PlotLegends → {"Cₙ, n=1,...,5"}]}],
 {{n, 5}, 1, 5, 1}, ControlType → None]
```

Figure 7

```
Manipulate[Plot[{Cot[ντ], Aτ/(ντ)}, {ντ , 0, 2 Pi},
   AxesLabel → {"ντ"}, PlotRange → {{0, 3}, {-3, 3}},
   PlotStyle → {{Thick, ColorData["HTML"]["RoyalBlue"]},
     {Thick, ColorData["HTML"]["DarkGreen"]}},
   PlotLegends → {"ctg(ντ)", "Aτ/(ντ)"}, ImageSize → 150],
  {{Aτ, -1}, -1, -5, ControlPlacement → Left,
   ImageSize → Tiny}, ControlPlacement → Left]
```

Figure 9

```
Manipulate[Module[{a = 8, m = 10, p = 6, B = 3, Vmax = 7,
    sol = NDSolve[{c'[t] == p - B Vmax c[t] c[t - τ]^m/(a^m + c[t - τ]^m),
       c[t /; t ≤ 0] == 40}, c, {t, -1, 10}]},
   Plot[Evaluate[c[t] /. First[sol]], {t, -1, 10},
    AxesLabel → {"t", "c(t)"},
    PlotStyle → {Thick, ColorData["HTML"]["RoyalBlue"]}]],
  {{τ, 0.15}, 0.1, 1}, FrameLabel → "τ=0.15",
  SaveDefinitions → True]
```

Figure 10-14

```
Manipulate[
 Block[{ c, u, t},
  A = (D[p - b Vmax x y^m/(a^m + y^m), x] /. {x -> eq}) /. {y -> eq};
  B = (D[p - b Vmax x y^m/(a^m + y^m), y] /. {y -> eq}) /. {x -> eq};
  eq = c /. FindRoot[p - b Vmax c c^m/(a^m + c^m) == 0, {c, 1}][[1]];
  sol = First[c /. NDSolve[
      {c'[t] == p - b Vmax c[t] c[t - τ]^m / (a^m + c[t - τ]^m),
       c[t /; t ≤ 0] == IC}, c, {t, 0, T}]];
  sollin = First[u /. NDSolve[{u'[t] == A u[t] + B u[t - τ],
       u[t /; t ≤ 0] == IC - eq}, u, {t, 0, T}]];
  imagesize = ImageSize → {300, 300}; pr = {eq + z, eq - z};
  fr = Frame → {True, True, False, False};
  coleq = ColorData["HTML"]["OrangeRed"];
  collin = ColorData["HTML"]["DarkRed"];
  colsol = ColorData["HTML"]["RoyalBlue"];
  TabView[
   {Text[Style["t vs. c(t)"]] →
     Show[
      Plot[{sol[t], eq}, {t, 0, T},
       PlotRange → pr,
       PlotStyle → {{colsol, Thick}, {coleq, Thick, Dashed}},
       PlotLegends → Placed[{"c(t)", "eq"}, Above]],
      If[cb, Plot[eq + sollin[t], {t, 0, T}, PlotRange →
          {{0, T}, {-10, 10}}, PlotStyle → {collin, Thick},
         PlotLegends → Placed[{"u(t)"}, Above]], Graphics[]],
      fr, FrameLabel -> {t, c[t]}, imagesize],
    Text[Style["c(t) vs. c(t-τ)"]] →
     Show[
      Graphics[{PointSize[0.03], coleq, Point[{eq, eq}]}],
      ParametricPlot[{sol[t], sol[t - τ]},
       {t, 1, T}, PlotStyle → {colsol, Thick},
       PlotLegends → Placed[{"(c(t),c(t-τ))"}, Above]],
      If[cb, ParametricPlot[{eq + sollin[t], eq + sollin[t - τ]},
        {t, 1, T}, PlotStyle → {collin, Thick}, PlotLegends →
         Placed[{"(u(t),u(t-τ))"}, Above]], Graphics[]],
      PlotRange -> {pr, pr}, fr, FrameLabel ->
       {c[t], c[t - τ]}, imagesize],
```

```
    Text[Style["c(t) vs. c(t-τ) vs. c(t-2τ)"]] ->
     Show[
      Graphics3D[
       {PointSize[0.03], coleq, Point[{eq, eq, eq}]}],
      ParametricPlot3D[{sol[t], sol[t - τ], sol[t - 2 τ]},
       {t, 1, T}, PlotStyle → {colsol, Thick}, PlotLegends →
        Placed[{"(c(t),c(t-τ),c(t-2τ))"}, Above]],
      If[cb, ParametricPlot3D[{eq + sollin[t],
          eq + sollin[t - τ], eq + sollin[t - 2 τ]},
         {t, 1, T}, PlotStyle → {collin, Thick}
         , PlotLegends → Placed[{"(u(t),u(t-τ),u(t-2τ))"},
           Above]], Graphics3D[]],
      PlotRange -> {pr, pr, pr}, Axes → True,
      AxesLabel -> {c[t], c[t - τ], c[t - 2 τ]}, imagesize]
  }, Dynamic[pos]]],
Style["Solution curve", 12, Bold], Delimiter,
Text[Style["Nonlinear equation", Bold, 11]],
{{a, 8, "a"}, 1, 10,
 Appearance → "Labeled", ImageSize → Tiny},
{{b, 3, "b"}, 2, 4, Appearance → "Labeled", ImageSize → Tiny},
{{m, 5, "m"}, 4, 8, Appearance → "Labeled", ImageSize → Tiny},
{{p, 6, "p"}, 5, 7, Appearance → "Labeled", ImageSize → Tiny},
{{Vmax, 7, "Vmax"}, 6, 8,
 Appearance → "Labeled", ImageSize → Tiny}, Delimiter,
Control[{{cb, True, Text[Style["Linear equation", Bold, 11]]},
  {True, False}, ControlType → Checkbox}],
PaneSelector[{True → Row[{Row[{"                          ",
       "A", " ", Dynamic[A]}], "\n",
     Row[{"                              ", "B",
       " ", Dynamic[B]}]}],
  False → Row[{" "}]}, Dynamic[cb]], Delimiter,
Text[Style["Parameters of solution", Bold, 11]],
{eq, Appearance → "Labeled", ImageSize → Tiny},
{{IC, 5, "Initial value"}, 1, 40,
 Appearance → "Labeled", ImageSize → Tiny},
{{z, 5, "Zoom"}, 5, 0.1, Appearance → "Labeled",
 ImageSize → Tiny},
{{τ, 0.25, "Delay"}, 0, 0.5,
 Appearance → "Labeled", ImageSize → Tiny},
{{T, 5, "Time"}, 2, 10, Appearance → "Labeled",
 ImageSize → Tiny},
ControlPlacement → Left, SaveDefinitions → True]
```

Declaration

Undersigned Eliza Bánhegyi certify that the content of this thesis is my own work using only the referred sources. I take notice that my thesis will be placed at the library of University of Szeged between the loanable books and it may be published on the internet.

Szeged, 10^{th} May 2014

....

Eliza Bánhegyi

Összefoglaló: A Cheyne-Stokes légzés késleltetett modelljének számítógépes vizsgálata

Bánhegyi Eliza

Bolyai Intézet, Természettudományi és Informatikai Kar
Szegedi Tudományegyetem

A Cheyne-Stoke légzés egy embereket veszélyeztető légzési betegség, mely az általános légzésminta változásával mutatható ki. Ilyenkor az amplitúdó, ami közvetlenül összefügg a légzési térfogattal, a ventilációval, szabályosan emelkedik és csökken minden periódusban, periódusonként átmeneti légzés kimaradással megszakítva. Ekkor a légzésenkénti térfogat rendkívül alacsony *(1. ábra)*.

Először is szükségünk van néhány fiziológiai tényre a modellünkhöz. Az artériás szén-dioxid szintet (CO_2) - jelölje $c(t)$- receptorok ellenőrzik melyek meghatározzák a légcsere mértékét. Ezek a CO_2-érzékelő receptorok az agytörzsben helyezkednek el, tehát van egy velejáró késés - jelölje τ -, az egész légzésszabályzó rendszerben. Tudjuk, hogy a légcsere reakciógörbéje a CO_2-ra szigmoid alakú. Tegyük fel, hogy a V légcsere függése c-től közelítőleg leírható az úgy nevezett Hill-függvénnyel, ahol $V_{\max}$ a maximális légzési kapacitás, a paraméter a és a Hill együttható m pozitív konstansok, melyek kísérletileg meghatározottak.

Tegyük fel, hogy a CO_2 kiürülése a vérből arányos a légcsere és a vérbeli CO_2 szint szorzatával. Legyen p a CO_2 állandó metabolikus termelődése a testben. Ekkor a CO_2 szint változása modellezhető a

$$\frac{d\,c(t)}{dt} = p - b\,V_{\max}\,c(t)\,\frac{c^m(t-\tau)}{a^m + c^m(t-\tau)}$$

egyenlettel, ahol b egy pozitív paraméter, mely szintén kísérleti adatokból meghatározható. A τ késés a tüdőbeli vér oxigénellátása és az agytörzsi kemoreceptorok érzékelése között eltelt idő.

Első lépéseként átparaméterezünk, bevezetjük a dimenziótlan mennyiségeket, hogy egyszerűsítsük a jelöléseket: $x'(t) = 1 - \alpha\,x(t)\,V(x(t-\tau))$. Keressük az egyensúlyi helyzetét a fenti egyenletnek. Mivel az $\frac{1}{\alpha\,x_0}$ monoton csökken 0-ba, a $V(x_0)$ monoton nő 1-be, amint $x_0 \to \infty$, így egyetlen pozitív egyensúlyi helyzet van (*3. ábra*).

Közönséges differenciálegyenletek esetén: legyen az $X'(t) = F(X(t))$ nemlineáris differenciálegyenlet rendszert. A megoldás explicit megadásához szükségünk van az egyensúlyi helyzeten kívül linearizálás módszerére. Legyen $X(t)$ az egyenlet megoldása, ekkor tekintsünk egy kis eltérést az egyensúlyi helyzettől

$X(t) = X_0 + U(t)$, ahol $U(t)$ kielégíti az $U'(t) = F(X_0^* + U(t))$ egyenletet. Most az $U(t) = 0$ körüli megoldásokra koncentrálunk. F-*et* az X_0 egyensúlyi helyzet körüli Taylor sorával közelítjük. Így kapunk egyrészt egy lineáris tagot másrészt a többi magasabb fokú tagot együttesen tekintve egy $O(U)$ nagyságrendű elhanyagolható tényezőt. Ekkor fennáll a linearizálás alaptétele ([3] p. 151):

◆ TÉTEL

Tekintsük az $X' = F(X)$ differenciálegyenlet rendszert ahol $F \in C^1$. Tegyük fel, hogy

1. $X(t)$ egy megoldása az $X' = F(X)$ rendszernek minden $t \in [\alpha, \beta]$ esetén valamint $X(t_0) = X_0$;

2. $U(t)$ a megoldása az $X(t)$ szerinti variációs egyenletnek, melyre $U(t_0) = U_0$;

3. $Y(t)$ az a megoldása az $X' = F(X)$ egyenletnek, melyre $Y(t_0) = X_0 + U_0$.

Ekkor

$$\lim_{U_0 \to 0} \frac{|Y(t) - (X(t) + U(t))|}{|U_0|} = 0$$

egyenletesen minden $t \in [\alpha, \beta]$ esetén.

Késleltetett differenciálegyenletek esetén hasonló a folyamat. Legyen $x'(t) = f(x(t), x(t-\tau))$ a linearizálni kívánt egyenlet $f(x_0, x_0) = 0$ egyensúlyi helyzettel. Jelölje u az egyensúlyi helyzettől való eltérést. Ekkor az f többváltozós Taylor sorba fejtése az (x_0, x_0) körül: $f(x, y) = f(x_0, x_0) + J(x_0).(u(t), u(t-\tau)) + O(u^2)$, ahol $J(x_0) = (\partial_x f, \partial_y f)(x_0, x_0)$.

A fenti módszert az átparaméterezett egyenletre alkalmazva kapjuk, hogy $u'(t) = A\,u(t) + B\,u(t-\tau)$, ahol $A = -\alpha\, V(x_0)$, $B = -\alpha\, x_0\, V'(x_0)$. A megoldást $u(t) \propto e^{\lambda t}$ alakban keressük, ekkor a karakterisztikus egyenlet a következő: $\lambda = A + B\, e^{-\lambda \tau}$. A közönséges esettel ellentétben megszámlalhatóan végtelen sok karakterisztikus gyököt kapunk, melyeknek nincs véges torlódási pontja (*5. ábra*).

Vizsgáljuk meg közelebbről az általános $u'(t) = A\,u(t) + B\,u(t-\tau)$ egyenletet. A karakterisztikus gyököket $\lambda = \mu + i\,\nu$, alakba írva az Euler formula segítségével kapjuk: $\mu = A + B\, e^{-\mu\tau} \cos \nu\tau$, $\nu = -B\, e^{-\mu\tau} \sin \nu\tau$. $\mu = 0$-t rögzítve vizsgáljuk a stabilitási görbéket A és B függvényében. Ezek mentén tiszta képzetest karakterisztikus gyököket kapunk. Az $u = 0$ egyensúlyi helyzet stabilitására vonatkozó tétel a következő ([2] p. 53):

◆ TÉTEL

(a) Ha $A + B > 0$ *, akkor* $u = 0$ *instabil.*

(b) Ha $A + B < 0$ *és* $B \geq A$*, akkor* $u = 0$ *aszimptotikusan stabil.*

(c) Ha $A + B < 0$ *és* $B < A$ *, akkor létezik* $\tau_c > 0$ *úgy, hogy* $u = 0$ *aszimptotikusan stabil, ha* $0 < \tau < \tau_c$ *és instabil, ha* $\tau > \tau_c$*.*

A (c) fennállásakor létezik egy tisztán képzetes gyökpár $\tau_c = \frac{1}{\sqrt{B^2 - A^2}} \frac{1}{\cos\left(-\frac{A}{B}\right)}$ *esetben.*

Mivel egy oszcilláló természetű betegséggel foglalkozunk, minket azon paramétertartományok érdekelnek, ahol az egyensúlyi helyzet instabil, különösképpen azok, ahol a növekvő oszcilláció előreláthatólag korlátos ciklikus viselkedésű. Meg kell határoznunk a paraméterek bifurkációs értékét, ahol $\mathrm{Re}\,\lambda = 0$. Emiatt a karakterisztikus egyenlet megoldása rögzített $\mu = 0$ mellett $\mathrm{ctg}\,\nu\tau = \frac{A\tau}{\nu\tau}$, ahol $\frac{\pi}{2} < (\nu\tau)_1 < \pi$.

Ezt visszahelyettesítve az Euler formulával kapott egyenletekbe a bifurkációs feltétel $-B\tau = \sqrt{\left((-A\tau)^2 + (\nu\tau)_1{}^2\right)}$. Ha ez az egyenlőség nem áll fenn, azaz $-B\tau < \sqrt{\left((-A\tau)^2 + (\nu\tau)_1{}^2\right)}$, akkor az egyensúlyi helyzet lokálisan és globálisan is aszimptotikusan stabil. A kísérleti eredmények paramétereit figyelembe véve a kritikus késés $\tau = 0.25$ perc. Ezen analitikus eredmények hasonlóak a légzőszervi megbetegedések komplexebb modelljeihez. A megfigyelt Cheyne-Stokes légzés periódusa 2-3-szorosa a becsült késésnek.

A 10-14 összetett interaktív ábra lehetőséget ad az olvasónak további megfigyelésekre különböző paraméterek, kezdeti érték, késés és idő függvényében. $\tau = 0$ késéssel mind az eredeti, mind a linearizált egyenlet monoton tart az egyensúlyiheyzetbe. A kezdeti feltétel határozza meg a monoton növekvést illetve csükkenést, ekkor közönséges differenciálegyenlettel van dolgunk. A késést növelve az egyensúlyi helyzet körüli oszcillálás után aszimptotikus stabilitás figyelhető meg. A kezdeti érték ekkor az oszcilláció amplitúdóját és hosszát határozza meg. A kritikus késést túllépve korlátos periodikus viselkedés következik az eredeti egyenletnél. Együtt indulnak a görbék, majd időben egyre jobban eltávolodnak egymástól, a linearizált egyenlet megoldása instabil.